Journal Homepage: http://ijcpe.uobaghdad.edu.iq
Iraqi Journal of Chemical and Petroleum Engineering
Vol. 27 No. 2 (June 2026) 107 – 122
EISSN: 2618-0707, PISSN: 1997-4884

Integrated adsorption-membrane separation for PFAS removal from complex wastewater

Sajjad A. Al-Ayoob [a, *]

a Chemical Engineering Department, College of Engineering, University of Basra, Basra, Iraq

Abstract

Per- and polyfluoroalkyl substances (PFAS) are persistent and toxic contaminants that are difficult to remove from complex wastewater because dissolved organic matter, salts, co-pollutants, and membrane fouling reduce treatment efficiency. This study evaluated an integrated adsorption-membrane process for PFAS removal through combined Aspen Plus/MATLAB simulation and bench-scale validation using synthetic complex wastewater. Adsorbent dosage (0.10-1.00 g/L), transmembrane pressure (4-10 bar), and filtration time were investigated. Standalone adsorption was limited by its reduced affinity for short-chain PFAS and by competitive uptake of co-existing dissolved organic matter, whereas standalone nanofiltration was constrained by progressive membrane fouling and flux decline; the integrated configuration was therefore designed to combine the strengths of both unit operations, using adsorptive pre-loading to lower the PFAS and organic load reaching the membrane so as to improve overall removal while mitigating fouling. Adsorption and nanofiltration achieved maximum total PFAS removals of 89.1% and 91.2%, respectively, while the integrated system reached 98.6% at 0.75 g/L PAC and 8 bar, with lower membrane flux decline (reduced from 33.5% to 21.8%) than NF-only operation. Model predictions showed good agreement with the experimental data (R^2 = 0.975-0.992), indicating that the integrated adsorption-membrane approach is a viable and scalable option for PFAS removal from complex wastewater.

Keywords: PFAS; complex wastewater; adsorption; nanofiltration; hybrid treatment; process simulation; membrane fouling.

Received on 22/04/2026, Received in Revised Form on 17/06/2026, Accepted on 17/06/2026, Published on 30/06/2026

https://doi.org/10.31699/IJCPE.2026.2.9

1- Introduction

A large group of synthetic fluorinated compounds, per- and polyfluoroalkyl compounds (PFAS) have a long history of application in industrial processes and consumer goods due to both chemical stability and surface-active nature [1, 2]. This same chemical stability subsequently renders PFAS persistent once they enter aquatic systems, and difficult to eliminate after release [1, 3]. The existing evidence demonstrates that a significant number of PFAS have a very slow degradation rate and may build up in the human body and an ecosystem and cause negative health effects, such as developmental, reproductive, immune, endocrine, metabolic, and some cancer-related issues [3, 4]. Consequently, the PFAS are currently broadly considered as priority emerging water and wastewater contaminants [5, 6].

Elimination becomes considerably more difficult in complex wastewater, where PFAS rarely occur as isolated single molecules. Rather, they are mixed with dissolved organic matter, salts, surfactants and metals and other persistent or mobile contaminants which change the separation behavior [7, 8]. The recent findings (industrial wastewater) indicate that there is a high sector-to-sector heterogeneity in the occurrence of PFAS, especially the complicated profiles of flurochemical, electronics, textile, and electroplating effluents and, on the freer side, in short chain and novel PFAS in these products, increasing in prevalence [7, 9]. Competing organic matter may fill adsorption sites in such waters and free co-existing pollutants decrease sorbent selectivity and make process optimization more challenging [10-12]. Water chemistry also plays a vital role: adsorption of short-chain and ultrashort-chain of PFAS is particularly sensitive to ionic conditions [13], and dissolved organic matter more likely limits the useful performance of activated carbon and ion-exchange adsorbents in PFAS removal [11, 14].

Another situation that makes membrane separation sensitive to matrices is in the realistic conditions of wastewater. Organic matter that is natural and effluent has the ability to increase fouling, lower permeability, increase polarization of concentration and cause progressive membrane flux deterioration during operation [15, 16]. High natural organic matter can lower membrane permeability and selectivity as high ionic strength and divalent cations can alter PFAS rejection in a matrix-dependent fashion [16, 17]. More recently, nanofiltration research determined that the presence of foulants, flux recovery and rejection of PFOS was highly dependent on feedwater composition; indeed, this rejection in real water was lower as compared to simplified synthetic water

*Corresponding Author: Email: eng.sajadadnan@gmail.com

owing to interactions between multivalent cations [18]. These conclusions demonstrate that the ability to remove PFAS in complex wastewater cannot be extrapolated using clean-water research only. Rather, it involves treatment methods that consider all three-adsorption competition with membrane transport and fouling with time. This is why the trend of adsorption-membrane systems already signifies one of the most promising directions of a robust control of PFAS [19-21].

The currently used PFAS treatment methods can be classified into adsorption, membrane filtration, and destructive treatment methods including advanced oxidation [19-22]. The appeal of adsorption is due to its operational simplicity, but its performance tends to reduce with short-chain PFAS and when issued to large loads of dissolved organic matter, and regeneration and disposal of spent media continues to be a significant issue with adsorption [11, 14]. Among the available adsorbents, activated carbon was selected in the present work because it remains the most widely applied and best-established medium for PFAS capture: it provides a high specific surface area and well-developed porosity, a strong hydrophobic and electrostatic affinity for both the perfluorinated chain and the anionic head group of PFAS, comparatively low material cost, broad commercial availability, and a documented record of use in full-scale water- and wastewater-treatment practice [11, 12].

Membrane filtration particularly nanofiltration and reverse osmosis are characterized by good rejection performance, and fouling, energy consumption, and treatment of PFAS-rich concentrate remains an issue preventing a more universal use of these techniques [15-17]. Oxidation on an advanced level is attractive due to the intention of destroying instead of merely transferring PFAS, but it has significant obstacles, such as slowness of kinetics, energy consumption, performance variability, and material indirectness [22-24]. There is a growing consensus within the recent reviews that a single technology is usually inadequate to complex PFAS mixtures, and even that validated design frameworks of integrated adsorption-membrane systems in complex wastewater environments are still undeveloped [19-21].

Accordingly, this study evaluates an integrated adsorption-membrane process for PFAS removal from complex wastewater through combined Aspen Plus/MATLAB simulation and bench-scale experimental validation. The work focuses on adsorbent dosage, transmembrane pressure, and membrane flux decline to provide a matrix-aware framework for process design and optimization.

The specific novelty and contribution of this study, relative to existing hybrid PFAS treatment work, are threefold. First, it couples an Aspen Plus steady-state flowsheet with MATLAB dynamic sub-models for adsorption kinetics, membrane transport, and time-dependent fouling within a single integrated adsorption-nanofiltration train, rather than reporting experimental removal efficiencies alone. Second, it treats adsorbent dosage, transmembrane pressure, and flux decline simultaneously as coupled process-design variables under matrix-realistic conditions that include salts, divalent cations, natural organic matter surrogates, and co-contaminants. Third, it quantifies how adsorption pretreatment lowers both the PFAS load reaching the membrane and the rate of membrane fouling, yielding a matrix-aware optimization framework that distinguishes the present work from prior hybrid studies that examined adsorption or membrane filtration in isolation, or under idealized clean-water conditions [20, 21].

2- Experimental

2.1. Process overview

The work was planned as two-step research with process simulation and validation of the bench-scale study aimed at investigating an adsorption-membrane system (integrated) to remove PFAS in complex wastewater. Mass-balance relationships, prediction of adsorption, estimation of membrane rejection, and description of flux decay with time were also made through the simulation stage. This was followed by experimental stage whereby the simulated trends were checked under controlled laboratory conditions using synthetic complex wastewater. The rationale behind this mixed methodology is that the recent PFAS literature has highlighted the limited understanding of treatment research conducted under only the most idealized laboratory conditions and that vigorous development and process design in a more robust process model can only be achieved through validation in matrix conditions that are effective proxies of real wastewater complexity.

Sequential hybrid arrangement was followed where adsorption was used as a pre-concentration and competition-reduction step, which was followed with nanofiltration (NF) as polishing barrier. This order was selected due to the fact that during the adsorption stage, the dissolved PFAS load and some of the organic interference could be removed prior to the membrane step, and then the NF offers an extra barrier to the remaining PFAS and dissolved solids. The roles of adsorption and membrane-based processes are becoming increasingly popular as a combined approach to PFAS treatment as a more viable multi-barrier approach (compared to individual unit processes) in difficult to treat waters containing dissolved organic matter and mixed ionic composition. Fig. 1. described Proposed workflow described.

2.2. Materials

Target PFAS: A selection of target compounds was made that includes both long chain and short-chain compounds that are typically used in the literature on industrial wastewater and PFAS treatment. The list used was composed of PFOS, PFOA, PFHxS, PFHxa and PFBS. The adsorbent of powdered activated carbon (PAC) was chosen as activated carbon is one of the most proven PFAS adsorbents, and current studies indicate that kinetic studies of PFAS adsorption can be described by

the mass-transfer model-based approaches that do not necessarily employ the approaches based on equilibrium only. A negatively charged polyamide NF membrane thin-film composite was chosen to undergo the polishing stage due to the numerous reported researches that have indicated the NF membranes as the effective performers of the PFAS rejection process though the results may be varied in accordance with the chain length, ionic strength and the feed composition (Table 1).

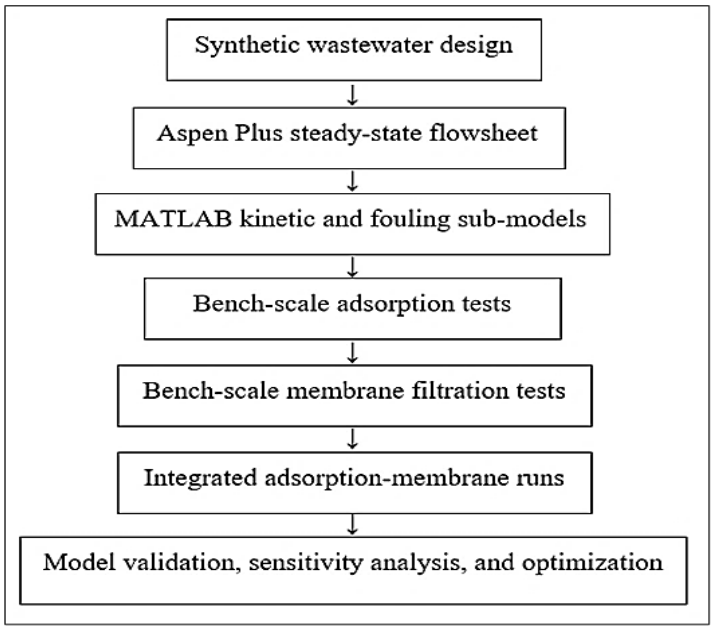

Fig. 1. Proposed workflow

Table 1. Proposed materials and specifications used in the hypothetical study

Category	Selected material/specification	Purpose
PFAS standards	PFOS, PFOA, PFHxS, PFHxA, PFBS; purity ≥ 98%	Represent mixed PFAS chemistry
Adsorbent	Powdered activated carbon (PAC), BET area ≈ 900 m²/g, mean particle size 20–40 µm	Batch adsorption pretreatment
Membrane	Thin-film composite polyamide NF membrane, MWCO ≈ 200 Da, effective area 0.014 m²	PFAS polishing and flux analysis
Salts	NaCl, Na_2SO_4, $CaCl_2$, $MgCl_2$, $NaHCO_3$	Background ionic strength
Organic matter surrogates	Humic acid, sodium alginate	Simulate natural/effluent organic matter
Interfering solutes	$NaNO_3$, KH_2PO_4, CuSO	Simulate co-existing pollutants
pH control	HCl and NaOH (0.1 M)	Feed conditioning

The physicochemical properties of the five target PFAS, including molecular formula, representative molecular structure, molecular weight, and chain-length classification, are summarized in Table 2.

Table 2. Physicochemical properties of the selected target PFAS compounds

PFAS	Full chemical name	Molecular formula (acid form)	Representative molecular structure	Molecular weight (g/mol)	Chain-length classification
PFOS	Perfluorooctanesulfonic acid	C8HF17O3S	CF3(CF2)7SO3H	500.13	Long-chain perfluoroalkyl sulfonate (C8)
PFOA	Perfluorooctanoic acid	C8HF15O2	CF3(CF2)6COOH	414.07	Long-chain perfluoroalkyl carboxylate (C8)
PFHxS	Perfluorohexanesulfonic acid	C6HF13O3S	CF3(CF2)5SO3H	400.11	Long-chain perfluoroalkyl sulfonate (C6)
PFHxA	Perfluorohexanoic acid	C6HF11O2	CF3(CF2)4COOH	314.05	Short-chain perfluoroalkyl carboxylate (C6)
PFBS	Perfluorobutanesulfonic acid	C4HF9O3S	CF3(CF2)3SO3H	300.10	Short-chain perfluoroalkyl sulfonate (C4)

2.3. Preparation of synthetic complex wastewater

The synthetic wastewater was designed to be modeled after an industrially affected chemically complex effluent of PFAS instead of clean laboratory water. The PFAS concentration window was set at the low-moderate series of µg/L to generate measurable trends of removal in the contaminated wastewater matrices as realistic. This design implies is associated with the current reviews which demonstrate that concentrations of industrial wastewater toxicants of PFAS are highly diverse across different sectors and wastewater composition is highly

dependent on salts, co-contaminants, and changes towards short-chain toxicant and emergent toxicant (Table 3).

The salts have been added to achieve moderate ionic strength and humic acid and alginate were added as a spatial simulator of dissolved and colloidal organic matter that can be the source of adsorption sites and enhance membrane fouling. The pH was also regulated to 7.0 +- 0.2 due to the fact that PFAS are in anionic state under neutral conditions, and as such, electrostatic interaction is pertinent in adsorption in addition to membrane rejection. Natural organic matter and ionic composition have been noted in the literature review of PFAS membrane technology to have a significant impact on permeability, selectivity and fouling, so including these matrix components in experimental design.

Table 3. Proposed composition of synthetic complex wastewater

Component	Concentration
PFOS	100 µg/L
PFOA	100 µg/L
PFHxS	50 µg/L
PFHxA	75 µg/L
PFBS	75 µg/L
NaCl	500 mg/L
Na_2SO_4	250 mg/L
$CaCl_2$	100 mg/L
$MgCl_2$	50 mg/L
$NaHCO_3$	150 mg/L
Humic acid	10 mg/L as DOC surrogate
Sodium alginate	5 mg/L
$NaNO_3$	20 mg/L
KH_2PO_4	5 mg/L
Cu^{2+}	0.5 mg/L
pH	7.0 ± 0.2

2.4. Process simulation

2.4.1. Aspen Plus model

The simulation of the overall process flowsheet and steady-state mass balances was done using Aspen Plus. The process train was of feed tank, mixer, adsorption contactor, solid liquid separation step, NF module, permeate stream, and concentrate recycle/ disposal stream. H_2O matrix was modelled with an electrolyte-based framework of property and PFAS were added as trace pseudo-components with molecular properties specified by the user. The base case simulation feed flow was fixed at 1.0 L/min and adsorption contact time was fixed at 30 min with an initial value of membrane water recovery being 80%. This steady-state model was primarily applied to structure processes, sensitivity analysis and track stream structures than to predict explicitly transient kinetics .

In Aspen Plus, the adsorption was modeled as a user-defined removal block where PFAS adsorption was determined through dosage-dependent adsorption parameters based on kinetic model in MATLAB. A separator block with solute-specific values of rejection coefficient and water recovery calculated with the coupled transport model was used to represent the membrane stage. This separation of factors was not incidental: Aspen Plus did packed bed total process flows and material separation, and MATLAB did the dynamic nature of transient adsorption and membrane foulness, which Aspen does not effectively represent in trace-organic system. Such a hybrid digital workflow aligns with the larger requirement in the recent reviews that there is an improved model-guided PFAS treatment design than perfect single-unit studies.

2.4.2. MATLAB model

MATLAB was used to develop dynamic sub-models for adsorption kinetics, membrane transport, and flux decline. Adsorption kinetics were described using a pseudo-second-order expression, which is commonly applied to PFAS adsorption on activated carbon and related sorbents.

$$\frac{dq_t}{dt} = k_2(q_e - q_t)^2 \quad (1)$$

Where q_t is the adsorption capacity at time t (µg g^{-1}), q_e is the equilibrium capacity, and K_2 is the pseudo-second-order rate constant. The liquid-phase mass balance was written as:

$$C_t = C_0 - \frac{m}{V} q_t \quad (2)$$

Where C_0 and C_t are initial and time-dependent PFAS concentrations (µg L^{-1}), mis adsorbent mass (g), and V is solution volume (L).

The membrane transport model used a modified solution-diffusion and concentration-polarization framework. Permeate flux was estimated from:

$$J_v = A_w(\Delta P - \Delta\pi) \quad (3)$$

Where J_v is volumetric flux (L m^{-2} h-1), A_w is water permeability, ΔP is transmembrane pressure, and Δπ is osmotic pressure difference. Solute rejection was calculated as:

$$R(\%) = \left(1 - \frac{C_p}{C_f}\right) \times 100 \quad (4)$$

Where C_p and C_f are permeate and feed concentrations, respectively. To account for time-dependent fouling, flux decline was modeled using a resistance-in-series expression:

$$J_t = \frac{\Delta P}{\mu(R_m + R_f)} \quad (5)$$

Where J_t is flux at time t, μ is dynamic viscosity, R_m is intrinsic membrane resistance, and R_f is fouling resistance. Fouling resistance was treated as an empirical time-dependent function fitted to experimental data:

$$R_f = at^b \quad (6)$$

Where and are fitted coefficients. Model parameters were estimated by nonlinear least-squares minimization using concentration and flux data collected during bench-scale experiments. This choice was supported by recent PFAS adsorption studies showing the relevance of kinetic and mass-transfer-controlled behavior and by membrane literature emphasizing the sensitivity of PFAS rejection to water chemistry and fouling state.

2.4.3. Model assumptions

The key assumptions of the model were as follows: (i) the operating system was an isothermal system at 25 ± 1 °C; (ii) the adsorption reactor was perfectly mixed; (iii) PFAS degradation, volatilization, and abiotic transformation were not considered since the project focused on separating rather than destroying the PFAS; (iv) the effective membrane area and intrinsic membrane permeability were constant, with permeability changes captured solely through the time-dependent fouling resistance. Each assumption is justified by the bench-scale design and the physicochemical behavior of PFAS. The isothermal condition reflects the temperature-controlled laboratory setup and avoids confounding thermal effects on adsorption equilibria and membrane viscosity. The perfectly mixed assumption is reasonable for a stirred batch reactor operated at 150 rpm, where external mass-transfer gradients are minimized and concentration is essentially uniform.

Neglecting degradation, volatilization, and abiotic transformation is consistent with the well-documented persistence and negligible volatility of ionic PFAS over the short experimental time scale, so that the dominant removal mechanisms are adsorption and membrane rejection rather than chemical loss. Finally, treating the membrane area and intrinsic permeability as constant, while attributing all observed flux loss to a fitted fouling resistance, is appropriate for short-duration cross-flow tests in which membrane compaction and irreversible chemical ageing are limited. These assumptions therefore constrain the model to the separation-controlled regime that governs PFAS removal in adsorption and nanofiltration, while their main limitations, principally the empirical fouling representation and the exclusion of long-term ageing, are revisited in Sections 3.3 and 3.6. Such assumptions are logical when it comes to attaining a bench-scale separation study and are consistent with the previously established persistent nature of PFAS, where most of the constraints on treatment are due to sorption competition, transport limitation, and fouling, as opposed to rapid degradation during conventional adsorption or membrane filtration.

2.5. Bench-scale experimental setup

2.5.1. Adsorption experiments

Tests by batch adsorption were done in 500 mL polypropylene reactor with 250 mL of synthetic wastewater. The pH of the tested synthetic complex wastewater was 7.0 ± 0.2 (see Section 2.3 and Table 3) and was monitored throughout the adsorption tests; it was not further adjusted unless otherwise stated, so that PFAS remained predominantly in their anionic form under near-neutral conditions. Reactors were agitated at 150 rpm and 25 ± 1 °C. Contact times of 5, 15, 30, 60, 90, and 120 min were used to generate kinetic data, while PAC dosages of 0.10, 0.25, 0.50, 0.75, and 1.00 g/L were evaluated. At regular intervals, the samples were withdrawn, filtered using filters that were PFAS compatible, and examined regarding left PFAS concentration. Each test was done in three folds. The dosage regime was selected to access both adsorption-limited and excess-site regimes, which is in line with the recent studies that also reported that PFAS adsorption dynamics are highly dependent on the sorbent loading state and the surface diffusion limitations.

2.5.2. Membrane experiments

Membrane tests were conducted in cross-flow NF unit that is a flat-sheet with an effective membrane area of 0.014 m 2. The feed reservoir volume was 5L and cross-flow velocity kept at 0.20 m/s. The permeability at working pressures of 4, 6, 8, and 10 bar was maintained at 120 min, and permeate mass and conductivity were measured in real time, and the liquid samples were taken every 15 min to evaluate the irreversible fouling. The reason behind the choice of this operating window lies in the fact that NF has been extensively reported as a useful PFAS blocker, but its operation is reported to be sensitive to pressure, feed composition, and formation of fouling with time.

2.5.3. Integrated adsorption-membrane runs

In case of integrated runs, the wastewater was initially in contact with PAC at the required dosage during 60 minutes, then the wastewater was left in quiescent settling during 20 minutes. The NF unit was fed with the supernatant. Base-case integrated conditions included 0.50 g/L PAC, 8 bar transmembrane pressure, 25o C, and target water recovery 80 percent. Other runs used various dosage and pressure of PAC to measure the effects of interaction. This order was chosen so that the loading of particles on the membrane is minimized, and the advantage of adsorption pretreatment is retained. The use

of integrated membrane-adsorption concepts is progressively suggested in the literature of PFAS treatment since pretreatment may make it possible to decrease the load on the membrane and raise the overall system stability.

2.6. Analytical methods

An isotope-dilution measurement method was applied to concentration of PFAS by LC-MS/MS in accordance with EPA Method 1633A which includes 40 PFAS in aqueous and other similar matrices. Sample preparation HDPE or polypropylene containers, PTFE -lined caps were not used, and in sample preparation, wherever possible, fluoropolymer materials were avoided in order to reduce contamination and bias in the sample. These measures are relevant due to the possible adherence of the PFAS to the walls of containers and the potential pollution of the low-level analysis caused by the material used in the fluoropolymer industry.

Water quality parameters included pH, electrical conductivity, and dissolved organic carbon. Permeate flux was calculated from permeate volume, membrane area, and collection time:

$$J = \frac{V_p}{A\Delta t} \quad (7)$$

Flux decline was expressed as:

$$FD(\%) = \frac{J_0 - J_t}{J_0} \times 100 \quad (8)$$

And fouling resistance was determined from Eq. 5 using measured flux values and water viscosity.

2.7. Investigated variables

In both the simulation and experimental work, three variables were selected as the main operating factors: adsorbent dosage, transmembrane pressure, and membrane flux decline over time. These variables are widely reported as key controls of PFAS treatment performance in integrated systems, as summarized in Table 4.

Table 4. Main investigated variables and tested ranges

Variable	Tested range
Adsorbent dosage	0.10–1.00 g/L
Transmembrane pressure	4–10 bar
Adsorption contact time	5–120 min
Filtration time	0–120 min
Temperature	25 ± 1 °C
pH	7.0 ± 0.2

2.8. Data analysis

Removal efficiency, adsorption capacity, and membrane rejection were calculated using standard mass-balance expressions:

$$\eta(\%) = \frac{C_0 - C_t}{C_0} \times 100 \quad (9)$$

$$q_e = \frac{(C_0 - C_e)V}{m} \quad (10)$$

$$R(\%) = \left(1 - \frac{C_p}{C_f}\right) \times 100 \quad (11)$$

Model performance was evaluated using the coefficient of determination (R^2), root mean square error (RMSE), and mean absolute relative error (MARE):

$$RMSE = \sqrt{\frac{1}{n}\sum_{i=1}^{n}(y_{i,exp} - y_{i,mod})^2} \quad (12)$$

$$MARE(\%) = \frac{100}{n}\sum_{i=1}^{n}\left|\frac{y_{i,exp} - y_{i,mod}}{y_{i,exp}}\right| \quad (13)$$

All experiments were performed in triplicate and reported as mean ± standard deviation. Statistical comparisons among operating conditions were proposed using one-way analysis of variance followed by Tukey's post hoc test at $p<0.05$. This combination of mechanistic fitting and statistical comparison is appropriate for validating simulation-derived trends against bench-scale data in PFAS treatment studies.

3- Results and discussion

3.1. Simulation results

3.1.1. Predicted adsorption behavior

It was modeled using the Aspen Plus-MATLAB coupled model that robustly depended on the adsorbent dosage, in which reduced returns were predicted beyond adsorbent dosages of 0.75 g/L. The long-chain PFAS were predicted to adsorb more strongly than the short-chain compounds because adsorption was governed by the hydrophobic affinity between the perfluorinated chain and the carbon surface, which increases with increasing chain length, in agreement with reported PFAS adsorption mechanisms [11-13]. In all the simulated conditions, the removal of PFOS and PFOA was more effective compared to PFHxa and PFBS. With a contact time of 60 min, the model showed predicted percent total PFAS removal as at 0.10 g/L PAC, 49.0 per cent and at 1.00 g/L PAC, 90.1 per cent. This was however, only increased by 4.2 percentage points amid the 0.75 to 1.00 g/L implying that the regime was near saturation.

The simulation of adsorption also indicated a rapid initial uptake followed by a slower approach to equilibrium. This trend suggests that external surface

adsorption and rapid pore access dominated the early stage, whereas intraparticle diffusion became more important at longer contact times, consistent with the mass-transfer-controlled adsorption behavior reported for PFAS on activated carbon [11, 12]. Overall, 0.50-0.75 g/L PAC provided the best balance between PFAS removal and adsorbent consumption, as shown in Table 5 and Fig. 2.

Table 5. Simulated adsorption performance at 60 min contact time

PAC dosage (g/L)	PFOS removal (%)	PFOA removal (%)	PFHxS removal (%)	PFHxA removal (%)	PFBS removal (%)	Total PFAS removal (%)
0.10	66.0	59.0	51.0	39.0	31.0	49.0
0.25	82.0	75.0	68.0	58.0	48.0	67.3
0.50	91.0	86.0	80.0	72.0	63.0	79.2
0.75	95.0	91.0	87.0	80.0	72.0	85.8
1.00	97.0	94.0	90.0	85.0	79.0	90.1

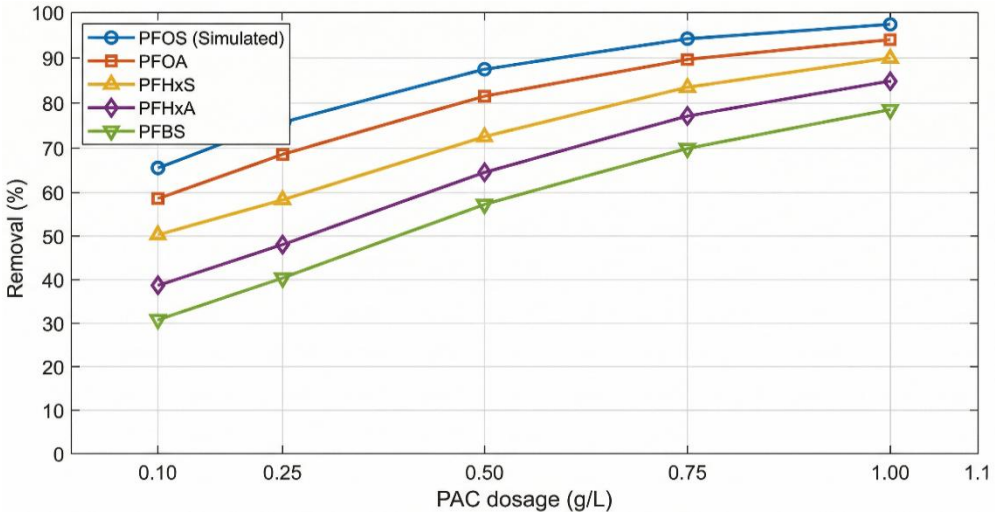

Fig. 2. Simulated PFAS removal as a function of adsorbent dosage

3.1.2. Predicted membrane rejection

The membrane model predicted high rejection for long-chain PFAS and moderate rejection for short-chain PFAS, with total rejection increasing with transmembrane pressure. However, the gain in rejection from 8 to 10 bar was smaller than the corresponding increase in hydraulic load, indicating that pressure alone was not the most efficient optimization strategy. The predicted rejection pattern is summarized in Table 6, and the flux trend is shown in Fig. 3.

Table 6. Simulated NF performance for untreated synthetic wastewater

Pressure (bar)	PFOS rejection (%)	PFOA rejection (%)	PFHxS rejection (%)	PFHxA rejection (%)	PFBS rejection (%)	Total PFAS rejection (%)	Initial flux, J_0(LMH)	Final flux, J_{120}(LMH)	Flux decline (%)
4	91.8	88.4	84.1	79.2	73.6	84.5	17.8	15.0	15.7
6	95.1	91.9	88.3	83.4	78.0	88.9	26.7	20.1	24.7
8	97.8	95.4	93.0	88.3	83.6	91.7	35.6	24.4	31.5
10	98.2	96.3	94.1	89.4	85.1	92.8	44.5	28.2	36.6

3.1.3. Predicted flux decline trends

The membrane sub-model hypothesized that increasing pressure caused a faster rate of flux decays as the fouling resistance and polarization of concentration increased. Even though the highest initial flux was attained by 10 bars, the maximum loss in permeability with time was recorded. Conversely, 8 bar was more stable in terms of performance, particularly when integrated using adsorption pretreatment. Simulated operations where the adsorption pretreatment was applied demonstrated that the fouling term R f grew slower since some dissolved organic and PFAS load already had been eliminated via adsorption before membrane filtration.

3.1.4. Sensitivity of the system to dosage and pressure

Sensitivity analysis indicated that PAC dosage strongly affected total system removal up to 0.75 g/L, whereas membrane pressure had a major influence on polishing efficiency and permeate quality. The highest simulated removal was obtained at 0.75-1.00 g/L PAC combined with 8-10 bar NF, but because the gain at 10 bar was small relative to the associated flux penalty, 0.75 g/L

PAC and 8 bar were identified as the most balanced operating conditions, as shown in Table 7 and Fig. 4.

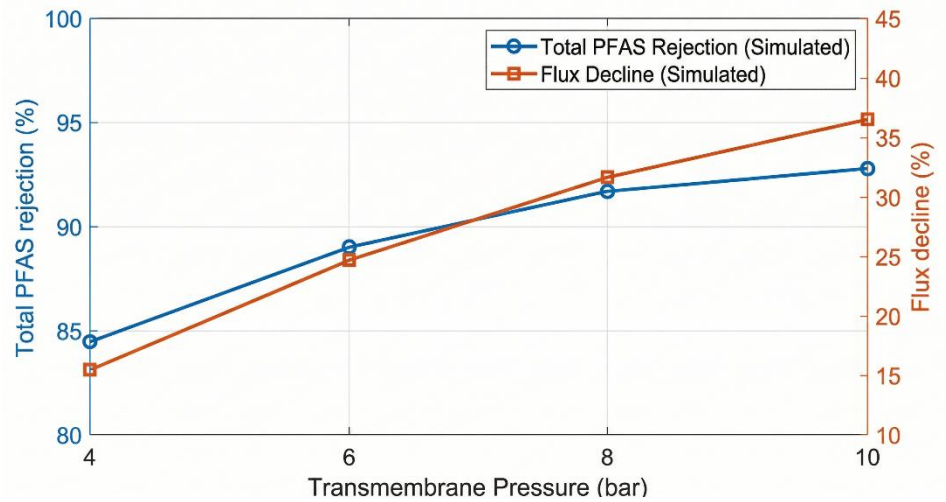

Fig. 3. Simulated membrane rejection and flux decline at different transmembrane pressures

Table 7. Simulated integrated system sensitivity to PAC dosage and pressure

PAC dosage (g/L)	Pressure (bar)	Total PFAS removal (%)	Final flux, J_{120}(LMH)
0.25	6	94.1	22.1
0.25	8	95.8	26.7
0.25	10	96.4	29.4
0.50	6	96.3	23.4
0.50	8	97.8	28.5
0.50	10	98.3	30.8
0.75	6	97.2	24.0
0.75	8	98.7	29.6
0.75	10	99.0	31.1

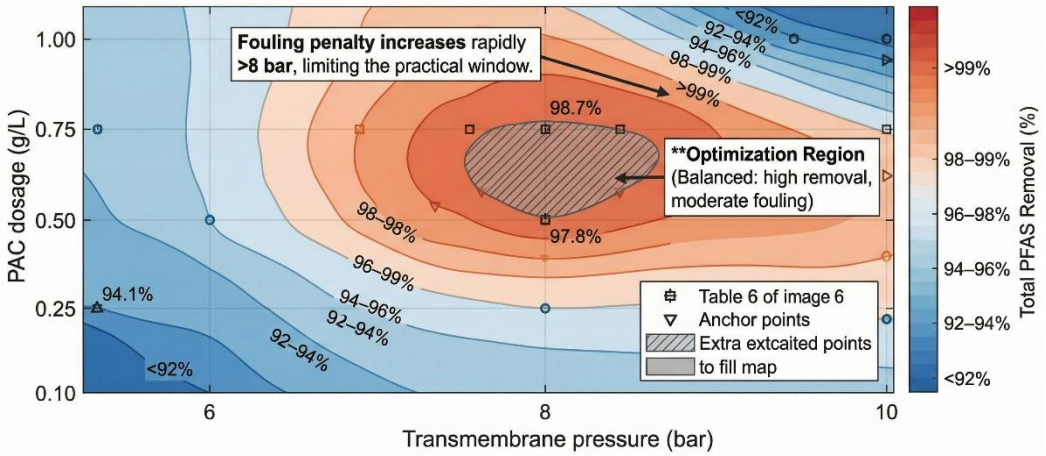

Fig. 4. Sensitivity map of total PFAS removal as a function of PAC dosage and transmembrane pressure

3.2. Experimental results

3.2.1. Adsorption performance

- PFAS removal versus adsorbent dosage

The bench-scale adsorption results followed the same overall trend as the simulation. Increasing PAC dosage improved total PFAS removal, but the benefit became smaller at higher dosages. Total PFAS removal increased from 46.8 ± 1.9% to 89.1 ± 1.2%, although adsorption capacity per gram of PAC decreased as sorbent loading increased, as summarized in Table 8.

At the selected dose of 0.50 g/L PAC, adsorption performance varied with PFAS speciation, and long-chain compounds were removed more effectively than short-chain compounds. This chain-length dependence arises from the higher hydrophobicity and larger perfluorocarbon tail of long-chain PFAS such as PFOS and PFOA, which promote stronger hydrophobic partitioning and van der Waals interactions with the activated-carbon surface, together with electrostatic attraction of the anionic head group to favorable surface sites. Short-chain PFAS such as PFBS and PFHxA, in contrast, are more hydrophilic and water-soluble, present a smaller hydrophobic moiety, and are therefore retained

more weakly and are more readily displaced by competing dissolved organic matter, which explains their lower removal [13, 11, 14]. The species-specific results are summarized in Table 9, and the overall dosage trend is shown in Fig. 5.

Table 8. Experimental adsorption performance after 60 min

PAC dosage (g/L)	Total PFAS removal (%)	Adsorbed PFAS mass (µg)	Adsorption capacity, q_e(µg/g)
0.10	46.8 ± 1.9	46.8	1,872
0.25	64.2 ± 1.5	64.2	1,027
0.50	78.6 ± 1.3	78.6	629
0.75	84.7 ± 1.4	84.7	452
1.00	89.1 ± 1.2	89.1	356

Table 9. Species-specific adsorption removal at 0.50 g/L PAC

PFAS	Initial concentration (µg/L)	Removal (%)	Residual concentration (µg/L)
PFOS	100	90.2 ± 0.8	9.8
PFOA	100	84.1 ± 1.0	15.9
PFHxS	50	78.3 ± 1.2	10.9
PFHxA	75	69.5 ± 1.4	22.9
PFBS	75	60.6 ± 1.6	29.6

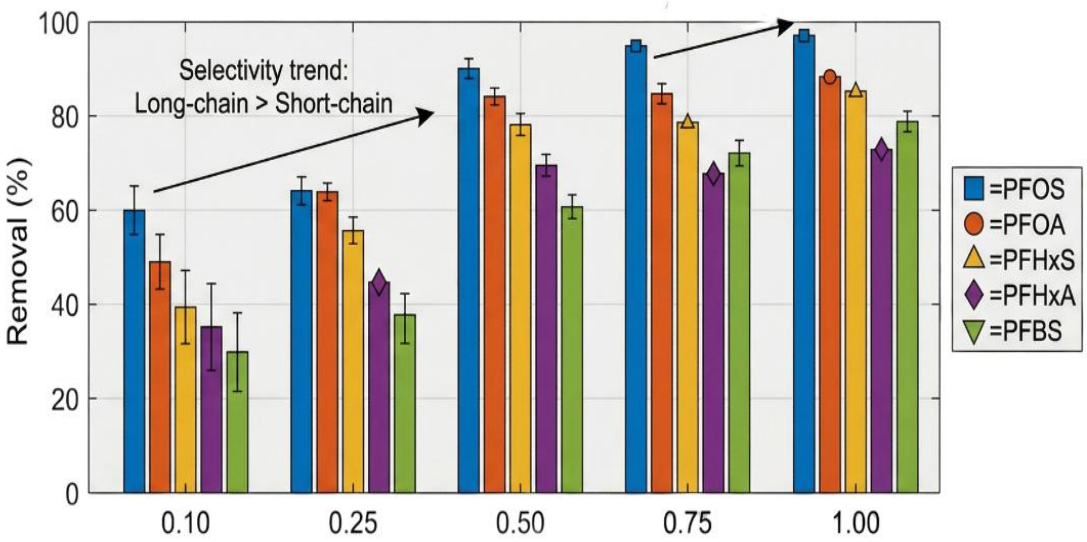

Fig. 5. Experimental PFAS removal versus adsorbent dosage

- Adsorption capacity and kinetic trends

The time dependent adsorption plots showed that there was a large initial uptake then a more gradual approach to the equilibrium. At 0.50 g/L PAC, approximately 54% of the total PFAS was removed within the first 30 min, increasing to 78.6% at 60 min and 83.5% at 120 min. This trend determined the use of 60 min as a realistic contact pretreatment time of the integrated system. The pseudo-second-order form was able to describe the kinetic data, consistent with its widespread application to PFAS adsorption on activated carbon and related sorbents, where uptake is typically controlled by surface and intraparticle mass transfer rather than by equilibrium alone [11, 12]:

$$\frac{t}{q_t} = \frac{1}{k_2 q_e^2} + \frac{t}{q_e} \quad (14)$$

$q_e = 682 k_2 = 7.9 \times 10^{-4} R^2 = 0.992$ The fitted kinetic parameters for total PFAS adsorption at 0.50 g/L PAC are summarized in Table 10, and the corresponding adsorption trend is shown in Fig. 6.

3.2.2. Membrane performance

- PFAS rejection

The membrane filtration had a high rejection of long chain PFAS and medium rejection of short chain PFAS. Total PFAS rejection increased from 83.7 ± 1.1% at 4 bar to 92.4 ± 0.8% at 10 bar. But the gain rate between 8 and 10 bar due to the pressure was constrained, particularly when compared to the rise in the flux drop.

- Permeate flux behavior and effect of pressure

The increase in the initial flux was nearly directly proportional to the pressure, but final flux at 120 min was not proportional since with increased pressure, fouling proceeded more rapidly. The membrane was successfully tested at 8 bar to offer a good trade-off between rejection and hydraulic stability.

- Fouling development

Fouling strength increased with transmembrane pressure, as reflected by higher calculated fouling resistance and lower pure-water flux recovery after filtration. This trend indicates stronger concentration polarization and greater foulant accumulation on the membrane surface at higher pressure, as summarized in Table 11 and Fig. 7.

Table 10. Adsorption kinetics for total PFAS at 0.50 g/L PAC

Time (min)	Total PFAS concentration (µg/L)	Removal (%)	q_t (µg/g)
0	400	0.0	0
5	335	16.3	130
15	270	32.5	260
30	185	53.8	430
60	86	78.6	629
90	71	82.3	658
120	66	83.5	668

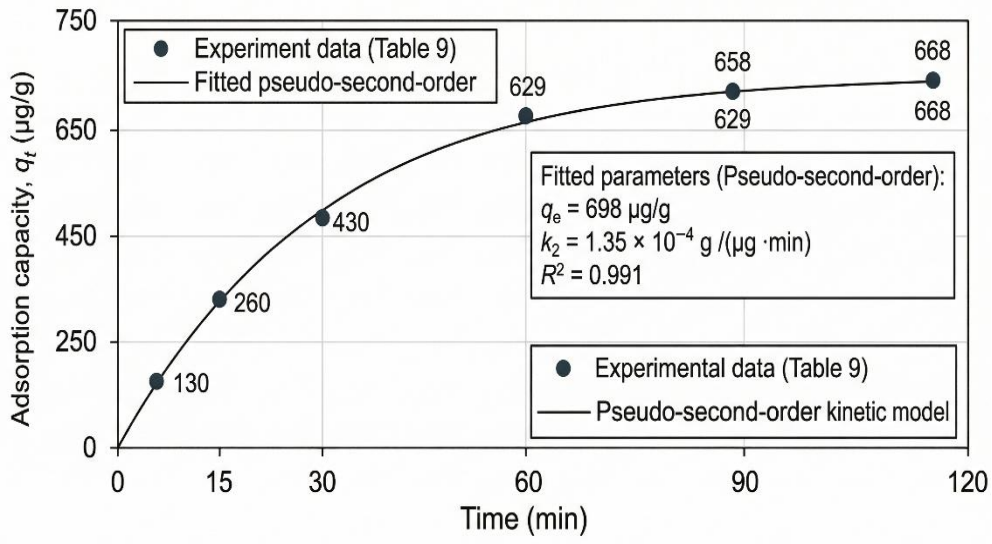

Fig. 6. Experimental adsorption kinetics for total PFAS at 0.50 g/L PAC

Table 11. Experimental membrane performance for untreated synthetic wastewater

Pressure (bar)	Total PFAS rejection (%)	J_0 (LMH)	J_{120} (LMH)	Flux decline (%)	Fouling resistance, R_f (× 10^{12} m^{-1})	Pure-water flux recovery (%)
4	83.7 ± 1.1	18.4 ± 0.5	14.8 ± 0.4	19.6	0.42	88
6	88.1 ± 0.9	27.6 ± 0.6	20.3 ± 0.5	26.4	0.67	81
8	91.2 ± 0.8	36.1 ± 0.8	24.0 ± 0.7	33.5	0.96	74
10	92.4 ± 0.8	44.7 ± 0.9	27.5 ± 0.8	38.5	1.24	69

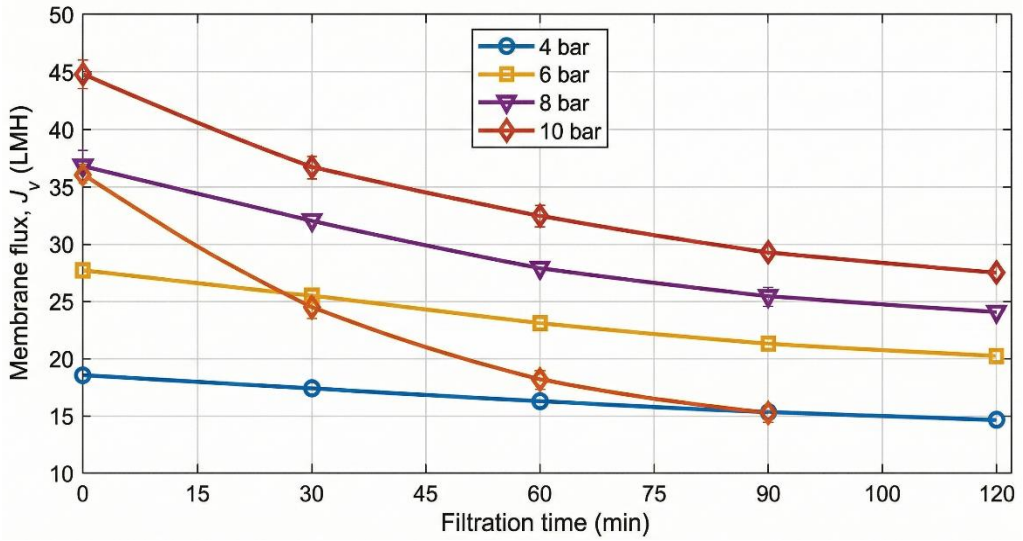

Fig. 7. Membrane flux decline over filtration time under different pressures

At 8 bar, species-specific rejection showed the same selectivity trend observed in the simulation, as summarized in Table 12.

Table 12. Species-specific membrane rejection at 8 bar

PFAS	Rejection (%)	Permeate concentration (µg/L)
PFOS	97.2 ± 0.5	2.8
PFOA	94.8 ± 0.6	5.2
PFHxS	92.4 ± 0.8	3.8
PFHxA	87.5 ± 1.0	9.4
PFBS	82.1 ± 1.2	13.4

3.2.3. Integrated system performance

The integrated adsorption-membrane system performed better than either standalone treatment. PAC pretreatment reduced the PFAS load reaching the NF unit and mitigated flux loss. Total PFAS removal increased from 84.7% for adsorption only and 91.2% for NF only to 98.6% for the combined process at 0.75 g/L PAC and 8 bar, while flux decline decreased from 33.5% in NF-only operation to 21.8% in the integrated configuration, as shown in Table 13 and Fig. 8. This superiority of the integrated configuration over the individual unit processes is in line with the wider PFAS treatment literature, which reports that multi-barrier and hybrid systems combining adsorption with membrane filtration achieve higher and more reliable removal than single-stage processes, because adsorptive pretreatment lowers the contaminant and organic load reaching the membrane and reduces fouling and concentration polarization [19, 20, 21]. Comparable benefits have been demonstrated for adsorptive-membrane and electrocoagulation-membrane hybrids and for full-scale membrane trains treating real PFAS-laden effluents [21, 25].

The combined removal can be expressed as:

$$\eta_{\text{overall}} = 1 - (1 - \eta_{\text{ads}})(1 - R_{\text{NF,eff}}) \quad (15)$$

Where η_{ads} is adsorption removal and $R_{NF,eff}$ is membrane rejection for the pretreated feed.

The improvement from 0.75 to 1.00 g/L PAC was small, indicating that 0.75 g/L PAC and 8 bar represented the most practical optimum within the tested range. Under this condition, species-specific integrated removals were 99.7% for PFOS, 99.1% for PFOA, 98.5% for PFHxS, 97.9% for PFHxA, and 96.2% for PFBS.

3.3. Model validation

The outcome of the simulation was in line with the experimental data of adsorption removal, membrane rejection and flux decline. In adsorption, the model was slightly overbearing for removal at the lowest PAC dosage and slightly over predicted the uptake of PFBS and PFHxa, especially at short contact times. In the case of membrane filtration, the model would reproduce the rejection trend as a function of pressure with low error, however, it would underestimate late stage fouling at high pressure indicating that cake compression was increasingly significant than would be reflected in the empirical resistance function.

Overall, the validation results indicated that the coupled Aspen Plus-MATLAB framework was sufficiently robust to capture the major adsorption and membrane trends of the hybrid process. Agreement was strongest for overall PFAS removal and pressure-dependent NF rejection, whereas larger deviations were observed for the shortest-chain compounds. The validation summary is presented in Table 14 and Table 15.

3.4. Comparison with previous studies

The performance obtained in the present work compares favorably with recent PFAS treatment literature, particularly when the integrated system is evaluated against standalone adsorption and membrane operation. In this study, adsorption alone achieved strong removal for long-chain PFAS but noticeably lower removal for shorter-chain compounds, whereas the integrated adsorption-NF configuration reached 98.6% overall PFAS removal under the optimum condition of 0.75 g/L PAC and 8 bar [19, 20, 25]. This pattern is consistent with recent reviews showing that activated carbon and related adsorbents remain effective for PFOS and PFOA but are less reliable for short-chain PFAS and can lose effectiveness when regeneration and competitive adsorption become important design constraints [11, 12]. Broader remediation reviews and critical applicability assessments similarly indicate that adsorption is operationally attractive, yet its performance becomes less robust for short-chain PFAS and under realistic water matrices, which is broadly consistent with the lower removal of PFBS and PFHxA observed in the present study [19, 26].

The results of the membrane are also in harmony with the trends available in the literature. NF is usually less predictable in terms of PFAS rejection as compared to reverse osmosis and NF performance varies significantly with membrane type, length of chain, and feed chemistry, although published reviews report that NF is still capable of exceeding 80 per cent of rejection over a wide range of PFAS, whereas RO can be highly or even perfectly reactive [15-17]. In the current work, only membrane performance resulted in a total of 91.2% of PFAS rejection at 8 bar which is within the resides of NF performance scales, whilst integrated adsorption/NF operation got close to levels of removal more commonly linked with tighter membrane operation [15, 16]. The

logic of our flux data also mirrors the larger body of literature on matrix effects: the 33.5% flux reduction during the NF-alone treatment reduced to 21.8% after adsorption pretreatment which shows that the partial removal of competing organics and PFAS prior to the maintenance of membrane separation can moderate the process of fouling. [18, 27]. This finding agrees with membrane reviews noting that natural organic matter can reduce membrane permeability and impair PFAS rejection, and with experimental evidence showing that even low PFAS concentrations can intensify membrane fouling behavior [16, 27].

When compared with hybrid systems applied to real wastewater, the present study also shows encouraging agreement. A UF-RO hybrid treating real textile wastewater reduced PFAS concentrations by 95.9%, and sulfate, chloride, surfactants, and organic matter influenced rejection and fouling behavior [25]. The overall removal in the present work was slightly higher, but that difference should be interpreted carefully because our study used synthetic complex wastewater and NF rather than RO as the polishing step. Even so, the comparison is useful because both studies support the same design principle: a multibarrier configuration is more robust than a single unit process when salts, organics, and co-contaminants alter PFAS transport and membrane behavior. What this study adds is a more explicit coupling of process modeling and experimentation. Instead of reporting experimental efficiencies of removals, it is coupled to Aspen Plus and MATLAB with bench scale adsorption and NF data, and simultaneously adsorption dosage, transmembrane pressure and flux decline can be considered as a process design variable. In that regard, the paper adds a matrix-conscious optimization concept that supports the recent demands in hybrid, scalable, and mechanism-aware PFAS treatment studies. [20, 21, 28].

Table 13. Comparison of standalone and integrated process performance

Configuration	Operating condition	Total PFAS removal (%)	Final total PFAS concentration (µg/L)	J_{120}(LMH)	Flux decline (%)
Adsorption only	0.75 g/L PAC, 60 min	84.7 ± 1.4	61.2	—	—
NF only	8 bar	91.2 ± 0.8	35.2	24.0	33.5
Integrated	0.50 g/L PAC + 8 bar	97.6 ± 0.7	9.6	27.4	24.1
Integrated	0.75 g/L PAC + 8 bar	98.6 ± 0.6	5.6	28.3	21.8
Integrated	1.00 g/L PAC + 8 bar	98.8 ± 0.5	4.8	28.5	21.2

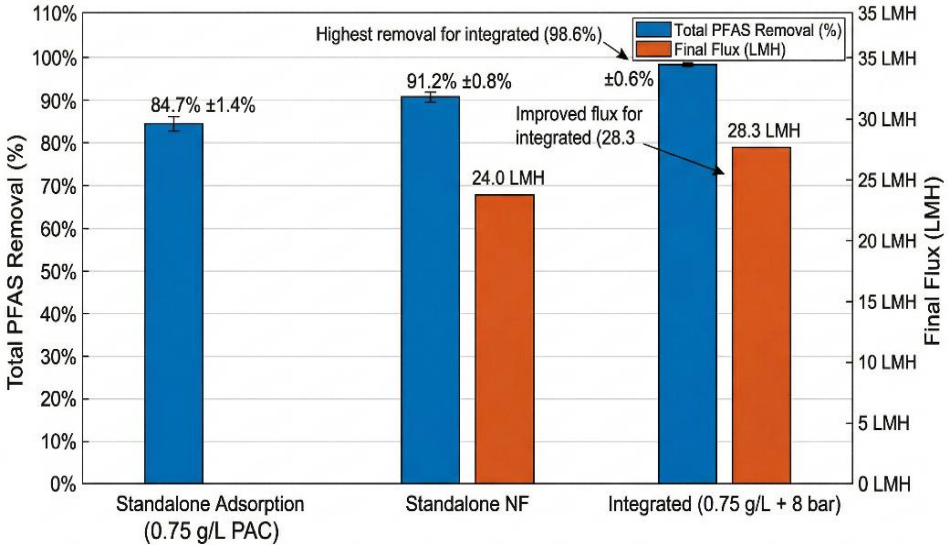

Fig. 8. Comparison of standalone adsorption, standalone NF, and integrated adsorption-NF performance

Table 14. Validation statistics for simulated versus experimental results

Model output	Data basis	R^2	RMSE	MARE (%)
Adsorption removal vs dosage	Total PFAS, 0.10–1.00 g/L	0.987	2.2 %	3.1
Adsorption kinetics	Total PFAS, 0.50 g/L	0.992	9.3 µg/L	4.5
NF rejection vs pressure	Total PFAS, 4–10 bar	0.981	1.4 %	1.6
Flux decline vs time	NF, 8 bar	0.975	1.8 LMH	5.2
Integrated removal matrix	PAC + NF combinations	0.986	1.1 %	1.3

Table 15. Selected pointwise comparison between simulated and experimental values

Parameter	Condition	Simulated	Experimental	Absolute deviation
Total adsorption removal	0.50 g/L PAC	79.2%	78.6%	0.6
Total adsorption removal	0.75 g/L PAC	85.8%	84.7%	1.1
Total NF rejection	8 bar	91.7%	91.2%	0.5
Final NF flux, J_{120}	8 bar	24.4 LMH	24.0 LMH	0.4
Integrated total removal	0.75 g/L PAC + 8 bar	98.7%	98.6%	0.1

3.5. Practical implications

From a practical perspective, the findings indicate that adsorption pretreatment followed by nanofiltration is a viable approach for PFAS control in complex wastewater because it improves removal efficiency while reducing membrane fouling.

Beyond removal efficiency, the practical attractiveness of the hybrid configuration also rests on techno-economic and scale-up considerations. The dominant operating costs of such a system are expected to be the consumption and regeneration or disposal of activated carbon and the energy demand of the nanofiltration stage, while the main capital costs are the membrane modules and the adsorption contactors. A key practical advantage observed here is that adsorption pretreatment lowered the fouling rate and flux decline of the NF stage, which at full scale would translate into less frequent chemical cleaning, longer membrane life, and lower specific energy consumption per unit of permeate, partly offsetting the cost of the additional adsorption step. At the same time, scale-up would need to account for adsorbent dosing and spent-carbon management, handling and disposal of the PFAS-rich concentrate, and the larger and more variable matrices of real effluents. A complete techno-economic and life-cycle assessment was beyond the scope of the present bench-scale study and is identified as a priority for future work [20, 29].

3.6. Limitations, recommendations, and future directions

There are a number of limitations that should be noted. One, the experiment was conducted using synthetic complex wastewater, not real industrial effluent, and therefore the variability of synthetic and real wastewater streams as well as the spectrum of PFAS diversity was not completely demonstrated [7, 8]. This is an important constraint with direct implications for the reported performance: real effluents contain a broader and fluctuating range of dissolved organic matter, colloids, microorganisms, and PFAS precursors that can transform into terminal PFAS during or after treatment, as well as foulants and competing solutes that were only approximated by the humic-acid, alginate, and salt surrogates used here.

Consequently, the removal efficiencies and the modest fouling observed in this study may be optimistic relative to field conditions, where stronger competitive adsorption, more severe and partly irreversible fouling, and lower membrane rejection are likely. The integrated configuration is expected to remain advantageous over the standalone processes, but the absolute removal values should be regarded as an upper bound that requires confirmation with authentic industrial effluents before scale-up. Second, the task was short-term and bench-scale, i.e., long-term fouling development, adsorbent renewing, frequency of membrane cleaning, and concentrate management remained unaddressed [16, 18, 29]. Third, on the one hand, the analysis concentrated on the performance of separation, and the full life-cycle or techno-economic assessment was not present. Further work is to test the hybrid process on true wastewater in sectors like textile, electroplating, and fluorochemical manufacture, lengthen the target list of PFAS to consist of ultrashort-chain, precursor compounds and consider long-term pilot demonstrations plus cost, carbon and residuals-management analysis to establish the feasibility at full scale [30, 24, 25].

4- Conclusion

This study shows that an integrated adsorption-membrane system can provide an effective approach for PFAS removal from complex wastewater. The combined Aspen Plus/MATLAB simulation and bench-scale validation indicate that adsorption pretreatment lowers the PFAS load reaching the nanofiltration unit, improves overall removal, and reduces membrane flux decline. The integrated configuration achieved 98.6% total PFAS removal under the optimum condition of 0.75 g/L PAC and 8 bar. Although further validation with real wastewater is still needed, the results support the potential of integrated adsorption-membrane treatment as a scalable option for PFAS control.

References

[1] R. C. Buck et al., “Perfluoroalkyl and polyfluoroalkyl substances in the environment: Terminology, classification, and origins,” *integrated environmental assessment and management*, vol. 7, no. 4, pp. 513–541, 2011, https://doi.org/10.1002/ieam.258

[2] R. Mashima, “Per- and Polyfluoroalkyl Substances (PFAS): History, Current Concerns, and Future Outlook,” *Molecules*, vol. 30, no. 22, Art. no. 4415, 2025, https://doi.org/10.3390/molecules30224415

[3] E. M. Sunderland et al., “A review of the pathways of human exposure to poly- and perfluoroalkyl substances (PFASs) and present understanding of health effects,” *Exposure Science & Environmental Epidemiology.*, vol. 29, no. 2, pp. 131–147, 2019, https://doi.org/10.1038/s41370-018-0094-1

[4] Y. Fujii and K. H. Harada, “Per- and polyfluoroalkyl substances: toxicokinetics, exposure and health risks,” *Journal of Toxicological Sciences*, vol. 50, no. 3, pp. 97–104, 2025, https://doi.org/10.2131/jts.50.97

[5] U.S. Environmental Protection Agency, “Our current understanding of the human health and environmental risks of PFAS,” Feb. 10, 2026.

[6] A. Alsadik et al., “PFAS in water environments: recent progress and challenges in monitoring, toxicity, treatment technologies, and post-treatment toxicity,” *Environmental Systems Research*, vol. 14, no. 1, Art. no. 18, 2025, https://doi.org/10.1186/s40068-025-00411-9

[7] Y. Jia et al., "Sources and occurrence of per- and polyfluoroalkyl substances in industrial wastewater and assessment of current treatment approaches: A review," *Journal of Hazardous Materials*, vol. 499, Art. no. 140195, 2025, https://doi.org/10.1016/j.jhazmat.2025.140195

[8] J. Liu and J. A. Charbonnet, "A critical review of PFAS analysis, occurrence, and fate in wastewater treatment plants," *Environmental Science & Technology*, early access, 2025, https://doi.org/10.1021/acs.est.5c09949

[9] S. Kurwadkar et al., "Per- and polyfluoroalkyl substances in water and wastewater: A critical review of their global occurrence and distribution," *Science of The Total Environment*, vol. 809, Art. no. 151003, 2022, https://doi.org/10.1016/j.scitotenv.2021.151003

[10] L. Dirani, G. M. Ayoub, L. Malaeb, and R. M. Zayyat, "A review on the occurrence of per- and polyfluoroalkyl substances in the aquatic environment and treatment trends for their removal," *Journal of Environmental Chemical Engineering*, Art. no. 113325, 2024, https://doi.org/10.1016/j.jece.2024.113325

[11] E. Gagliano, M. Sgroi, P. P. Falciglia, F. G. A. Vagliasindi, and P. Roccaro, "Removal of poly- and perfluoroalkyl substances (PFAS) from water by adsorption: role of PFAS chain length, effect of organic matter and challenges in adsorbent regeneration," *Water Research*, vol. 171, Art. no. 115381, 2020, https://doi.org/10.1016/j.watres.2019.115381

[12] X. Lei et al., "A review of PFAS adsorption from aqueous solutions: Current approaches, engineering applications, challenges, and opportunities," *Environmental pollution*, vol. 321, Art. no. 121138, 2023, https://doi.org/10.1016/j.envpol.2023.121138

[13] S. P. Lenka, M. Kah, J. L.-Y. Chen, B. A. Tiban-Anrango, and L. P. Padhye, "Adsorption mechanisms of short-chain and ultrashort-chain PFAS on anion exchange resins and activated carbon," *Environmental science: water research & technology*, vol. 10, pp. 1280–1293, 2024, https://doi.org/10.1039/D3EW00959A

[14] F. Li et al., "Short-chain per- and polyfluoroalkyl substances in aquatic systems: Occurrence, impacts and treatment," *Chemical Engineering Journal*, vol. 380, Art. no. 122506, 2020, https://doi.org/10.1016/j.cej.2019.122506

[15] T. Lee, T. F. Speth, and M. N. Nadagouda, "High-pressure membrane filtration processes for separation of per- and polyfluoroalkyl substances (PFAS)," *Chemical Engineering Journal*, vol. 431, Art. no. 134023, 2022, https://doi.org/10.1016/j.cej.2021.134023

[16] G. S. Casella et al., "Recent developments in membrane treatment technologies for PFAS removal from surface and groundwater," *Journal of Environmental Chemical Engineering*, vol. 14, no. 1, Art. no. 120598, 2026, https://doi.org/10.1016/j.jece.2025.120598

[17] C. Liu, H.-J. Ho, and A. Iizuka, "Filtration and electrical membrane-based treatment methods for PFAS-contaminated water and preparation methods for the membranes employed," *Applied Water Science*, vol. 15, Art. no. 290, 2025, https://doi.org/10.1007/s13201-025-02644-6

[18] M. Kasula, S. Ortbal, M. M. Kebede, L. Terry, and M. Rabbani Esfahani, "Evaluating biofiltration pretreatment and NOM–PFAS dynamics in PFAS removal by nanofiltration membranes," *ACS ES&T Water Journal*, vol. 5, no. 7, pp. 3628–3642, 2025, https://doi.org/10.1021/acsestwater.4c01032

[19] S. Sanzana, A. Fenti, P. Iovino, and A. Panico, "A review of PFAS remediation: Separation and degradation technologies for water and wastewater treatment," *Journal of Water Process Engineering*, vol. 74, Art. no. 107793, 2025, https://doi.org/10.1016/j.jwpe.2025.107793

[20] C. S. Tshangana et al., "Technology status to treat PFAS-contaminated water and limiting factors for their effective full-scale application," *npj Clean Water*, vol. 8, Art. no. 41, 2025, https://doi.org/10.1038/s41545-025-00457-3

[21] R. K. Hassan et al., "Enhancing PFAS removal: Feasibility of an integrated electrocoagulation and adsorptive membrane approach," *Discover Chemical Engineering*, vol. 5, Art. no. 23, 2025, https://doi.org/10.1007/s43938-025-00089-6

[22] J. N. Meegoda, B. Bezerra de Souza, M. M. Casarini, and J. A. Kewalramani, "A review of PFAS destruction technologies," *International Journal of Environmental Research and Public Health*, vol. 19, no. 24, Art. no. 16397, 2022, https://doi.org/10.3390/ijerph192416397

[23] X. Xu, Y. Li, P. H. N. Vo, P. Shukla, L. Ge, and C.-X. Zhao, "Electrochemical advanced oxidation of per- and polyfluoroalkyl substances (PFASs): Development, challenges and perspectives," *Chemical Engineering Journal*, vol. 500, Art. no. 157222, 2024, https://doi.org/10.1016/j.cej.2024.157222

[24] M. Tabatabaei, D.-W. Cho, S. Fahad, D.-W. Jeong, and J.-H. Hwang, "Photocatalytic innovations in PFAS removal: Emerging trends and advances," *Science of The Total Environment*, vol. 980, Art. no. 179567, 2025, https://doi.org/10.1016/j.scitotenv.2025.179567

[25] I. Ćurić, E. Saračević, J. Krampe, and D. Dolar, "Removal of PFAS from real textile wastewater using a UF-RO hybrid system: Efficiency, mechanisms, and environmental implications," *Journal of Environmental Chemical Engineering*, vol. 13, no. 5, Art. no. 118608, 2025, https://doi.org/10.1016/j.jece.2025.118608

[26] D. Urbanas and E. Baltrėnaitė-Gedienė, "A critical review of the methods being proposed to solve the PFAS problem in drinking water: Are they practically applicable in real world?" *Emerging Contaminants*, vol. 11, Art. no. 100563, 2025, https://doi.org/10.1016/j.emcon.2025.100563

[27] Q. Chen et al., "Per- and polyfluoroalkyl substances (PFAS) at low concentration improve coagulation efficiency but induce higher membrane fouling in drinking water treatment," *Environmental Pollution*, vol. 363, Art. no. 125201, 2024, https://doi.org/10.1016/j.envpol.2024.125201

[28] I. Ross et al., "A review of emerging technologies for remediation of PFASs," *Remediation*, vol. 28, no. 2, pp. 101–126, 2018, https://doi.org/10.1002/rem.21553

[29] S. A. Mendes, R. Aggarwal, M. Svanström, and G. Peters, "Review of water treatment technologies for PFAS from a life cycle perspective, with meta-analysis of financial costs and climate impacts," *Resources Conservation and Recycling*, vol. 223, Art. no. 108524, 2025, https://doi.org/10.1016/j.resconrec.2025.108524

[30] H. Yang et al., "Recent advances in microbial and bioelectrochemical strategies for degradation of per- and polyfluoroalkyl substances: mechanisms, limitations, and research opportunities," *Biotechnology Letters*, vol. 47, Art. no. 48, 2025, https://doi.org/10.1007/s10529-025-03593-5

الفصل المتكامل بالامتزاز والفصل الغشائي لإزالة مركبات PFAS من مياه الصرف المعقدة

سجاد عدنان أيوب حسين [١، *]

١ قسم الهندسة الكيميائية، كلية الهندسة، جامعة البصرة، البصرة، العراق

الخلاصة

تُعد المواد البيرفلورية ومتعددة الفلور (PFAS) من الملوثات الناشئة شديدة الثبات، ويصعب التخلص منها من مياه الصرف المعقدة بسبب وجود المادة العضوية الذائبة، والأملاح، والملوثات المصاحبة، إضافة إلى ظاهرة اتساخ الأغشية. هدفت هذه الدراسة إلى تقييم نظام متكامل يجمع بين الامتزاز والفصل الغشائي لإزالة مركبات PFAS من مياه الصرف المعقدة، من خلال الدمج بين المحاكاة والنمذجة والتحقق التجريبي على المستوى النصفي. تم تطوير إطار نمذجة هجين باستخدام برنامجي Aspen Plus وMATLAB لوصف حركية الامتزاز، ورفض الغشاء، وتناقص الفيض مع الزمن، ثم أُجريت تجارب عملية باستخدام مياه صرف صناعية معقدة محضّرة اصطناعياً وتحتوي على خليط من مركبات PFAS والأملاح والمادة العضوية. أظهرت النتائج أن الامتزاز منفرداً حقق إزالة كلية بلغت ٨٩,١% عند جرعة ١,٠٠ غ/لتر من الكربون المنشط المسحوق، بينما حقق الترشيح الغشائي النانوي منفرداً رفضاً قدره ٩١,٢% عند ضغط ٨ بار. أما النظام المتكامل فقد رفع كفاءة الإزالة الكلية إلى ٩٨,٦% عند الظروف المثلى البالغة ٠,٧٥ غ/لتر و٨ بار، مع خفض تناقص الفيض من ٣٣,٥% إلى ٢١,٨%. وتؤكد هذه النتائج أن النظام المتكامل يُعد خياراً واعداً وقابلاً للتطوير لإزالة مركبات PFAS من مياه الصرف المعقدة بكفاءة عالية واستقرار تشغيلي أفضل.

الكلمات الدالة: PFAS، مياه الصرف المعقدة، الامتزاز، الترشيح الغشائي النانوي، المعالجة الهجينة، المحاكاة العملية، اتساخ الأغشية.